

Gamma-Tocotrienol loaded liposomes as radioprotection from hematopoietic side effects caused by radiotherapeutic drugs

Sang-gyu Lee¹, Teja Muralidhar Kalidindi¹, Hanzhi Lou², Kishore Gangangari^{1,3}, Blesida Punzalan¹, Ariana Bitton⁴, Casey J. Lee⁴, Hebert A. Vargas¹, Soobin Park⁵, Lisa Bodei¹, Michael G. Kharas², Vijay K. Singh^{6,7}, Naga Vara Kishore Pillarsetty^{1,8*}, Steven M. Larson^{1,2,8*}

¹Department of Radiology, Memorial Sloan Kettering Cancer Center, New York, NY

²Molecular Pharmacology Program, Memorial Sloan Kettering Cancer Center, New York, NY

³Department of Chemistry, Hunter College, The City University of New York, New York, NY

⁴New York University, New York, NY

⁵Hunter College, New York, NY

⁶Department of Pharmacology and Molecular Therapeutics, F. Edward Hébert School of Medicine, Uniformed Services University of the Health Sciences, Bethesda, MD

⁷Armed Forces Radiobiology Research Institute, Uniformed Services University of the Health Sciences, Bethesda, MD

⁸Department of Radiology, Weill Cornell Medical College, New York, NY

Corresponding Author: Steven M. Larson, MD, Memorial Sloan Kettering Cancer Center, 1250 1st Ave, New York, NY 10065. Phone: 646-888-2212, Email: larsons@mskcc.org.

ORCID ID: <https://orcid.org/0000-0002-6111-7507>

*Contributed equally to this work

Key Words: Bone marrow, liposome, γ -tocotrienol, radiation protection

Running Title: Radioprotection of GT3-loaded liposome

Word Count: 4,978

Total Number of Figures: 4

Immediate Open Access: Creative Commons Attribution 4.0 International License (CC BY) allows users to share and adapt with attribution, excluding materials credited to previous publications.

License: <https://creativecommons.org/licenses/by/4.0/>.

Details: <http://jnm.snmjournals.org/site/misc/permission.xhtml>.



ABSTRACT

Rationale: With the successful development and increased use of targeted radionuclide therapy for treating cancer comes the increased risk of radiation injury to bone marrow—both direct suppression and stochastic effects, leading to neoplasia. Herein, we report a novel radioprotector drug, a liposomal formulation of gamma-tocotrienol (GT3), or GT3-Nano for short, to mitigate bone marrow radiation damage during targeted radionuclide therapy.

Methods: GT3 was loaded into liposomes using passive loading. [⁶⁴Cu]-GT3-Nano and ³H-GT3-Nano were synthesized to study the *in vivo* biodistribution profile of the liposome and GT3 individually. Radioprotection efficacy of GT3-Nano was assessed after acute ¹³⁷Cs whole-body irradiation at sublethal (4 Gy), lethal (9 Gy), or single high-dose [¹⁵³Sm]-EDTMP administration. Flow cytometry and fluorescence microscopy were used to analyze hematopoietic cell population dynamics and cellular site of GT3-Nano localization in spleen and bone marrow, respectively.

Results: Bone marrow uptake and retention of [⁶⁴Cu]-GT3-Nano was 6.98 ± 2.34 %ID/g, while [³H]-GT3-Nano uptake and retention was 7.44 ± 2.52 %ID/g at 24 h, respectively. GT3-Nano administered 24 hours before or after 4 Gy TBI promoted rapid and complete hematopoietic recovery, while recovery of controls stalled at 60%. GT3-Nano demonstrated dose-dependent radioprotection, achieving 90% survival at 50 mg/kg against lethal 9 Gy TBI. Flow cytometry of bone marrow indicated progenitor bone marrow cells MPP2 and CMP cells were upregulated in GT3-Nano-treated mice. Immunohistochemistry showed that GT3-Nano accumulates in CD105-positive sinusoid epithelial cells.

Conclusion: GT3-Nano is highly effective in mitigating marrow-suppressive effects of sub-lethal and lethal TBI in mice. GT3-Nano can facilitate rapid recovery of hematopoietic components in mice treated with the endoradiotherapeutic agent [¹⁵³Sm]-EDTMP.

INTRODUCTION

Radioiodine-131 therapy for well-differentiated thyroid cancer has played a seminal role in the creation of nuclear medicine as a medical sub-specialty and, for decades, was the only high-dose targeted radionuclide therapy (TRT) regimen considered standard of care in oncology. In the last 10 years, prospects for therapeutic nuclear medicine have been further enhanced by the addition of two successful new therapeutic radionuclides—for prostate cancer, Zofigo (Ra-223 Chloride), and for neuroendocrine tumors, Lutathera (Lutetium-177 Dotatate)—NDA-approved in 2013 and 2018, respectively. Key registry trials documented improved progression-free survival and these new therapeutic radiopharmaceuticals are now part of the standard pharmacopeia for advanced adult tumors.

The powerful combination of clinical success, commercial viability, and opportunity to satisfy a major unmet need for effective therapy of advanced solid tumors in adults and children now provides a powerful stimulus for the development of novel TRTs to stimulate further growth of the therapeutic arm of nuclear medicine. Examples of additional radionuclide-targeted therapies showing great promise for treatment of otherwise incurable tumors and in advanced clinical development include [¹⁷⁷Lu]-DKFZ-PSMA-617 for metastatic castration-resistant prostate cancer (in phase 3 testing through the multi-center “VISION” trial (1); iodine-131 ([¹³¹I]-NaI) re-induction therapy for radioiodine-refractory thyroid cancer (2); and [¹³¹I]-Omburtamab for CNS metastatic neuroblastoma in pediatric patients (3).

As the use of promising TRT agents expands, whole-body radiation doses will also increase, as will the probability of potentially dangerous side effects. These TRTs cause some degree of bone marrow suppression; this organ usually limits tumor dose escalation. E.g., reports on [¹⁷⁷Lu]-DOTATATE indicate that mild to moderate hematopoietic complications may be expected in the majority of patients, while severe grade 3/4 cytopenia occurs in a small but significant (11%) patient population and appears to be correlated with bone marrow dose (4,5). Myeloproliferative events, such as myelodysplastic syndrome

(MDS) and acute leukemia, have been reported in 2.35% and 1.1% of patients in a 30 (1-180)-month median follow-up (6). Similar considerations are postulated for other types of radionuclide therapies (7).

Radioprotectants (7) based on free radical scavenging capability have been developed over the past few decades to counteract the dangerous side effects of radiation. The radioprotector gamma-tocotrienol (GT3) is a vitamin E analog that has demonstrated highly potent radioprotection in mice and non-human primates (8). GT3 exerts its radioprotective effects by modulating multiple pathways, including inhibition of hydroxyl-methyl-glutaryl-coenzyme A reductase, inducing expression of the DNA repair gene RAD50, upregulation of thrombomodulin production, and progenitor cell mobilization, which facilitates hematopoietic recovery. However, due to hydrophobicity, GT3 is water-insoluble with poor bioavailability, making it unsuitable for human applications (9).

We have developed GT3-Nano, a radioprotector agent to mitigate hematopoietic effects after TRT and other forms of whole-body radiation. We developed a liposomal carrier for GT3 as a suitable drug formulation for practical solubilization and parenteral delivery of high-dose GT3, as required for optimal radioprotection. In prior work, by adjusting the size, zeta-potential, and PEG content, we discovered radiolabeled liposomal formulations that selectively target the spleen and bone marrow (SBMT-LIPO) with enhanced efficiency (10). For the purpose of radioprotection and radiotoxicity mitigation, we reasoned that SBMT-LIPO would be an ideal delivery vehicle because spleen and bone marrow are the primary sites of regenerative stem cells for hematopoietic recovery post-radiation. We hypothesized that a water-soluble formulation capable of delivering GT3 to the spleen and bone marrow would demonstrate enhanced radiation protection. In the current manuscript, we describe the synthesis, physicochemical characterization, and *in vivo* pharmacokinetics of GT3-Nano. The radioprotection properties of GT3-Nano against sub-lethal and lethal total body irradiation (TBI) as well as high-dose internal radiation with bone targeting [¹⁵³Sm]-EDTMP were evaluated in immunocompetent mice models and are presented here.

METHODS

All chemicals were used as received without further purification. All lipids and mini extruder were purchased from Avanti Polar Lipids (Alabaster, AL). The p-SCN-Bn-DOTA was purchased from Macrocyclics (Dallas, TX), and ^{64}Cu was purchased from Washington University in St. Louis (St. Louis, MO). GT3 was purchased from Chromadex (Irvine, CA) and tritium-labeled GT3 was synthesized at ViTrax (Placentia, CA). Mice were purchased from Envigo Laboratories (Indianapolis, IN).

Preparation of liposomes and characterization

Liposomes were prepared as previously described (10). Briefly, DSPC, cholesterol, succinyl-DPPE, mPEG2000-DSPE, and GT3 were mixed in chloroform, evaporated under N_2 flow, and lyophilized overnight. Lipid film was hydrated in PBS at 65 °C for 1 h and the lipid dispersion was extruded through 0.1 μm pore size Whatman[®] Polycarbonate Membrane Filter at 65 °C. Liposome size distribution and zeta potential at 25 °C in PBS pH 7.4 were determined by dynamic light scattering using Zetasizer Nano-ZS (Malvern, Worcestershire, UK). Further ^{64}Cu labeling was performed by adding [^{64}Cu]- CuCl_2 to the liposome at pH 5.5 with 0.2 M sodium acetate buffer at 50 °C. Reaction was monitored by ITLC-SG paper using 5 mM DTPA solution.

***In vitro* GT3 release from liposomes**

GT3-Nano liposomes containing different mole% of GT3 spiked with ^3H -GT3 (4 μCi) were placed inside a dialysis cassette with MWCO 50k and dialyzed against PBS. 100 μL of the liposomes were withdrawn at 0, 4, 20, 28, 44, 52, 68, and 140 h and transferred to a scintillation vial and mixed with 5 mL of Ecoscint A and the radioactivity was measured using a scintillation counter (Tricarb 2910 TR, PerkinElmer, Inc., Waltham, MA).

Biodistribution of ⁶⁴Cu liposome and ³H-labeled GT3-containing liposome

For biodistribution studies, approximately 5.5 MBq of [⁶⁴Cu]-DOTA-Bz-DSPE-labeled liposome and 0.74 MBq of [³H]-GT3-incorporated liposome was intravenously administered to C57/BL6 mice (n = 5 per group) via tail vein injection. Cohorts of mice were sacrificed at 24 and 48 h after injection. Major organs were collected and placed in pre-weighed culture tubes or Eppendorf tubes. For ³H activity measurement, major organs were collected in pre-weighed scintillation vials to which 500 μL of Soluene[®]-350 was added and incubated overnight incubation at 37 °C. 4.5 mL of Ecoscint A was added, mixed well, and counted in a scintillation counter.

***In vivo* efficacy of GT3 liposomes against total-body irradiation**

Six- to eight-week-old C57/BL6 mice were used for the whole-body irradiation studies. Cohorts of mice were intravenously administered with GT3-Nano (10 mg/kg, 6 mole%) either 24 h pre- or 24 h post-whole-body irradiation (4 Gy, Cs-135, dose rate = 82 cGy/min). Approximately 100 μL of blood was drawn using retro-orbital collection for complete blood cell count data at various time points up to 100 days post-radiation. For studies performed at AFRRRI (Bethesda, MD), 6- to 8-week-old male CD2F1 mice were housed in rooms with a 12-hour light and 12-hour dark cycle. The mouse holding room was maintained at 20-26 °C with 10-15 air exchange cycles per hour and a relative humidity of 30-70%. Mice were held in quarantine for one week and exposed to bilateral radiation in a ⁶⁰Co facility at a dose rate of 0.6 Gy/min.

Flow cytometry

Bone marrow cells were harvested by crushing the hind leg bones in a mortar with pestle in HBS + 2% FBS and passing through a 40 mm cell strainer. To measure hematopoietic stem and progenitor cell (HSPC) compartments, cells were stained with the appropriate cocktail containing antibodies specific for

lineage markers. The complete list of antibodies and markers are listed in **Supplemental Table 1**. Bone marrow cells were analyzed by a BD LSR Fortessa flow cytometer.

Immunohistochemistry

Seven-week-old C57/BL6 mice were injected with 100 μ L of bone marrow-targeting liposomes (NBD-SBMT-LIPO) incorporating fluorophore nitrobenzoxadiazole (NBD). Once euthanized, mice spleens were collected and embedded in optimal cutting temperature compound then snap frozen with dry ice. 10 μ m frozen spleen sections were collected on slides and washed three times with PBS followed by incubation with TBS+1% BSA solution for 1 hour. Sections were incubated with mouse anti-CD31 IgG and rabbit anti-CD105 IgG overnight at 4 °C. After washing primary antibody with PBS three times, the sections were incubated again with either goat anti-mouse IgG-Alex-647 or IgG-Alexa-594 for two hours at room temperature. Sections were mounted on slides and observed under fluorescence microscopy.

Institutional research approval

All animal experiments were approved by the Institutional Animal Care and Use Committee of Memorial Sloan Kettering Cancer Center under protocol #86-02-020 and Armed Forces Radiobiology Research Institute P2017-08-009.

RESULTS

Characterization of GT3-Nano formulation and GT3 release kinetics of ³H-labeled GT3-Nano

GT3 can be incorporated into bone marrow-targeting liposomes by adding up to 20 mole% GT3 in lipid mixture. ⁶⁴Cu labeling and stability of the colloidal suspension of GT3-Nano was measured and found to be nearly identical to bone marrow-targeting liposome (**Fig. 1**). The maximum loading capacity of GT3 in

SBMT-LIPO was determined by adding different amounts of GT3 into SBMT-LIPOs (**Fig. 1D**); 6, 10, 15, and 20 mole% of GT3 input were tested for liposomal formulation of GT3 for further studies.

Size distribution and negative surface charge play critical roles in high accumulation of SBMT-LIPO to bone marrow (*10*). Since GT3 incorporation into the lipid bilayer of SBMT-LIPOs modifies the surface property, zeta potential as well as size distribution have been determined (**Fig. 1B**). As shown in **Fig. 1B**, zeta potential of 10 mole% GT3-Nano is -14.4 mV, 2.4 mV higher than zeta potential of naïve SBMT-LIPO at pH 7.4. As shown in **Fig. 1D**, GT3 incorporation into SBMT-LIPO does not interfere with labeling of ^{64}Cu to DOTA-Bn-DSPE on GT3-Nano, which showed 100% labeling efficiency.

We prepared ^3H -GT3- GT3-Nano containing trace amounts of ^3H -GT3 as a surrogate for GT3 and measured the release of ^3H activity from the liposome using dialysis against PBS at different time points up to 140 h at room temperature. *In vitro* GT3 release was conducted to evaluate the physical stability of GT3 in GT3-Nano and tritium-labeled GT3 was used to measure release kinetics. As shown in **Fig. 1E and 1F**, the ^3H -GT3 release rate was measured by dialysis against PBS and 73–83% of ^3H -GT3 was retained in the liposome over 140 h of dialysis at room temperature.

Biodistribution of ^{64}Cu GT3-Nano and ^3H -labeled GT3-Nano showed similar accumulation pattern in spleen and bone marrow

Though the physicochemical changes are minimal, as shown in **Fig. 1**, the biodistribution of GT3-Nano must ensure that the formulation targets the spleen, liver, and bone marrow. We compared SBMT-LIPO, our liposomal radioprotectant, to the spleen and bone marrow. ^{64}Cu -labeled and ^3H -GT3 incorporated GT3-Nano were used to follow the liposomal distribution and GT3 distribution of 24 and 48 h after administration. As shown in **Fig. 2 and Supplemental Table 2**, bone marrow, spleen, and liver accumulations of GT3-Nano measured by [^{64}Cu]-GT3-Nano at 24 h are 12.48 ± 2.68 , 22.86 ± 8.14 , and 14.4 ± 1.1 %ID/g, respectively, and [^3H]-GT3-Nano at 24 h are 4.29 ± 3.22 , 7.95 ± 1.61 , and $6.53 \pm$

1.35 %ID/g, respectively, possibly related to differential metabolism of copper and GT3 in phagocytized materials.

GT3-Nano mitigates radiation effects by supporting faster and more complete recovery of white blood cells and lymphocytes after sublethal whole-body irradiation and [¹⁵³Sm]-EDTMP injection

As shown in **Fig. 3A**, 4 Gy whole-body radiation induced severe depletion of peripheral blood cells. White blood cells (WBC) and lymphocytes decreased to less than 10% of baseline counts with a nadir at day 1-4 post-irradiation, consistent with our previous reports (11). The rate of recovery of WBCs and lymphocytes in GT3-Nano treated groups (both pre- and post-) was faster, leading to >50% recovery by day 21 compared to untreated controls, for which recovery was about 20% by day 21. Both treated groups also demonstrated complete recovery of key parameters to baseline by day 43. For the untreated control group, WBC and lymphocyte counts recovered to about 60% at day 43 and we did not observe 100% recovery until day 99, at which points all the mice groups were euthanized. GT3-Nano treatment did not affect neutrophil, RBC, or platelet counts at 4 Gy whole-body irradiation (**Supplemental Figure 1**).

To evaluate the efficacy of GT3-Nano at a lethal dose of whole-body irradiation, C57/B6 mice (**Fig. 3B, left panel**) were first tested after irradiation with 9 Gy of ¹³⁷Cs. Following GT3-Nano treatment in the amount of 50 mg/kg, the survival rate of the mice was 80% at day 30, in contrast to a 0% survival rate in the untreated group at day 17 at the same irradiation level.

To test the dose dependency of survival with GT3-Nano treatment, CD2F1 mice were treated with 16, 24, 32, and 50 mg/kg of GT3-Nano and SBMT-LIPO (**Fig. 3B, right panel**). The difference between the survival of mice in the 16 and 24 mg/kg groups as compared to the group receiving SBMT-LIPO was not statistically significant. When compared to untreated mice (12), we do observe statistically significant differences between untreated controls and GT3-Nano groups at all doses. The survival of the mice in the

32 mg/kg treatment group at day 30 was 67% ($p < 0.05$) and in the 50 mg/kg group on the same day, it was 87% ($p < 0.05$). Thus, we confirm that GT3-Nano can rescue mice of two different strains from otherwise lethal radiation in a dose-dependent manner at two different institutions.

To test the ability of GT3-Nano to protect bone marrow from internal, exponential declining and continuous radiation with 1.93 day T-1/2, irradiation, mice were treated with [^{153}Sm]-EDTMP, a bone-targeting radiopharmaceutical commonly used as a bone pain palliation agent to treat pain caused by bone metastases of cancers. 50 mg/kg of GT3-Nano was administered 24 h prior to injection of 1.5 mCi [^{153}Sm]-EDTMP, followed by six injections of 50 mg/kg GT3-Nano over three weeks (days 1 and 4 of each week). As shown in **Fig. 3C**, GT3-Nano pre-treatment did not prevent the depletion of WBCs and lymphocytes and, as in untreated controls, the WBC and lymphocyte counts drop to 15% of baseline at day 4. Recovery of WBC is delayed until day 7 for both the GT3-Nano -treated and the control group. The nadir region continued to day 14 for the control group, while WBC counts of GT3-Nano started to recover at day 14. We found that the recovery of WBCs in the GT3-Nano -treated group was faster and more complete, reaching 88% over 99 days, while recovery of WBC counts in the control group reached 44% at day 21 and was still suppressed at time of sacrifice, day 99 ($p < 0.05$).

Flowcytometry shows faster and more complete recovery of the precursor hematopoietic cell populations in bone marrow, after injection of GT3-Nano

GT3 is known to inhibit hydroxy-methyl-glutaryl-coenzyme A reductase (HMGCR) and induce production of G-CSF and expression of DNA repair gene RAD50 as well as other unknown mechanisms (8,9). While uptake of GT3-Nano occurs in CD105⁺ endothelial cells, it is unclear which cell population is repopulated more rapidly in GT3-Nano treated group in the bone marrow.

Hematopoietic stem cells (HSCs) and multipotent progenitors (*13*) are responsible for replenishing other blood cells through the hematopoietic process, though HSCs mostly exist in a state of quiescence, or reversible growth arrest. The altered metabolism of quiescent HSCs helps the cells survive for extended periods of time. When provoked by cell death or damage, HSCs exit quiescence and begin actively dividing again (*13*). There are a number of markers that permit the prospective identification and isolation of HSCs and MPPs. HSC and MPP frequency changes in bone marrow were analyzed to identify which HSC/MPP subpopulations are protected by the GT3-Nano treatment. As shown in **Fig. 4A**), at day 14, myeloid-biased MPP subsets 2 (MPP2) and common myeloid progenitors (CMP) showed statistically significant increases in cell numbers during recovery in GT3-Nano treated groups, in comparison to other HSC subpopulations. While there is a general trend toward increased progenitor cell subpopulations in the GT3-Nano treated group, no statistically significant increases were observed in these other-HSPC populations (**Supplemental Figure 2**).

CD105 co-localization with fluorescently labeled SBMT-LIPO

As shown in **Fig. 4B**, NBD-SBMT-LIPO is primarily localized in endothelial cells lining the sinusoids within the red pulp region in the spleen, where sinusoids are engorged with blood and macrophages. CD105⁺ appears red on vascular and sinusoidal endothelial cells, where activated macrophages and monocytes are seen, with NBD-SBMT-LIPO co-localization. CD105⁺ cells are mainly localized in the red pulp region and some CD105⁺ cells are found in the white pulp region, where lymphocytes are abundant. CD31⁺ has been found on endothelial cells, platelets, macrophages and Kupffer cells, and lymphocytes. CD31⁺ cells in the spleen are mainly located in the marginal zone between the non-lymphoid red pulp and B cell-abundant white pulp. While abundant NBD-SBMT-LIPO colocalized with CD105⁺ cells, NBD-SBMT-LIPO also colocalized with CD31⁺/CD105⁺ cells (see arrows in **Fig. 4B**), which are known to produce IL-33 with radiation (*14*).

DISCUSSION

Particles such as liposomes, when introduced into the bloodstream, are rapidly cleared from the circulation by endothelial cells of the innate immune system in the liver, spleen, bone marrow, and lymph nodes (15). By modifying the composition of the liposomes, the liposome targets different organs (**Supplemental Figure 3**). The phagocytic endothelial cells of spleen and bone marrow line the blood vessels, which have a sinusoidal architecture that has adapted to allow blood cells to rapidly pass back and forth through holes in the vessel walls into adjacent cellular compartments. We reasoned that if we loaded liposomal particles with a known radiation mitigator/protector such as GT3, we could protect these sinusoidal endothelial cells as well as other essential stem cell types in the spleen and bone marrow that are responsible for restoration of hematopoietic function after radiation damage by TRT radiopharmaceuticals, as well as other types of acute radiation injury. The physical juxtaposition of the bone marrow niche for hematopoietic stem cells and progenitor cells within 10 microns of the sinusoids in bone marrow and spleen further supports this concept (16).

The studies reported in this paper demonstrate the efficacy of GT3 packaged liposomal formulations for the treatment of radiation-induced hematopoietic injury in mice. We employed both acute sub-lethal and lethal external beam radiation and high-dose ^{153}Sm bone-seeking radiation in mice to test efficacy. The principle benefits of therapy with GT3-Nano were more rapid and complete recovery of WBC at sublethal radiation (4 Gy external beam; ^{153}Sm overdose), which correlated with an increase in specific myeloid progenitor cells in the bone marrow. At supralethal radiation (up to 9.2 Gy), a dose response was observed for radiomitigation leading to “rescue” (survival) of 80-90% of mice with no detectable long-term effects after 100 days.

This work was predicated on prior studies that showed a strong link between hematopoietic cells and phagocytic sinusoidal endothelial cells in the bone marrow in both rabbits (17) and man (18). The two cell populations exist naturally in a homeostatic relationship. Radiation disrupts this relationship. At low

doses of radiation, the more sensitive hematopoietic cells were markedly suppressed, while the phagocytic cells were relatively unaffected. Over time, the homeostatic relationship was restored by the recovery of hematopoietic cells to baseline levels. At higher doses of radiation, both cell types were suppressed, although the time course of phagocytic cells' decline in function was much slower. Recovery of hematopoietic cells was restored only if the function of phagocytic cells was completely restored (6). More modern studies support this concept (19); Hooper et al stated, "We show that the extent and rate of sinusoidal endothelial cell regeneration after myelosuppression (post-radiation) dictate the rate of hematopoietic recovery."

Thus, protection of the human body from radiation exposure is a major unmet need for TRT, as well as other human endeavors such as space exploration and military and industrial applications, which are outside the scope of this paper. So far, bone marrow stimulants, such as lymphokines like filgrastim and derivatives provide valuable but limited support and more effective drugs are sorely needed (8). Storage forms must be stable to long-term storage in strategic national stockpiles and for use as needed with TRT, likely on the shelves of radiopharmacies. Herein, we report practical formulations of GT3-Nano with long-term stability. The carrier liposomes themselves are stable to physiochemical testing for two years when stored at 4 °C as a kit formulation (**Supplemental Figure 4 and 6**). The safety profile, well in excess of effective marrow-sparing doses, appears excellent, with no evident histopathology after doses above 100 mg/kg in mice (**Supplemental Figure 6**).

With regard to the mechanism of action, based on fluorescent tags on the liposomal particles, we determined that, as expected, specialized phagocytic cells of the innate immune system lining the sinusoids of bone marrow and spleen are the predominant sites of uptake and retention of these liposomes. GT3-Nano accumulates in these sinusoidal endothelial cells including CD105+ cells and CD31-expressing cells known to produce IL33 lymphokine, a peptide stimulus that activates stem cells and progenitor cells (14). In treated animals, we demonstrated increased MPP2 and CMP progenitor cell

populations in bone marrow. In preliminary studies, we have documented that at GT3-Nano doses effective for sub-lethal irradiation protection (10mg, GT3/kg), there is no reduction in efficacy of curative external beam treatment of human xenografts (**Supplemental Figure 7**). Since GT3-Nano shows efficacy in mitigating acute radiation effects, longer-term studies in humans are needed to determine impact on reduction of stochastic effects.

GT3-Nano affords radioprotection against both single high-dose rate gamma radiation delivered in 10 minutes with Cesium-137 source and slow dose rate beta radiation delivered exponentially in about 10 days by [¹⁵³Sm]-EDTMP. Both beta and gamma radiation cause most cellular damage by oxidative stress (20) and therefore it is not surprising that GT3-Nano can provide radiation protection against both types of radiation. However, it must be noted that repeated dosing was employed for radioprotection by GT3-Nano against [¹⁵³Sm]-EDTMP. Additional radiobiologic studies comparing and contrasting radiation protection mechanisms as a function of dose rate and mode of delivery are planned.

Conclusion

We have successfully developed GT3-Nano as a novel water-soluble liposomal drug delivery formulation of gamma-tocotrienol, a known ion scavenger drug. GT3-Nano selectively targets the spleen and bone marrow with high efficiency and provides radiation protection for progenitor stem cells against lethal whole-body radiation in mice models. GT3-Nano promotes more rapid hematopoietic recovery from high-dose radiation from both external sources as well as from the internal radiation emitter ([¹⁵³Sm]-EDTMP). We believe that GT3-Nano has major potential for the treatment of non-target bone marrow toxicities arising from whole-body radiation from external beam and targeted radiotherapeutics.

KEY POINTS

QUESTION: With the increasing use of targeted radionuclide therapy, novel approaches are needed to reduce non-target organ toxicity.

PERTINENT FINDINGS: By incorporating GT3 in SBMT-LIPO, GT3-Nano showed efficacy in blood cell increase and rescued mice from lethal dose of irradiation.

IMPLICATIONS FOR PATIENTS CARE: GT3-Nano is a potent radioprotectant that can potentially treat patients undergoing targeted radionuclide to facilitate rapid recovery of the hematopoietic function.

ACKNOWLEDGMENTS

Funding support from P30 CA008748 (NIH/NCI Cancer Center Support Grant), R01 CA201250-04, P50 CA086438 (SML), and MSKCC-IMRAS Seed Grant (SL, NP) is gratefully acknowledged. The study at the Armed Forces Radiobiology Research Institute was supported by intramural grant #RAB29173 to VKS.

DISCLOSURES

SL, NP, and SML are listed as the inventors on the intellectual property related to liposomes for delivering drugs to the spleen and bone marrow. The opinions or assertions contained herein are the private views of the authors and not necessarily those of AFRRI, the Uniformed Services University of the Health Sciences, or the Department of Defense.

FIGURES AND LEGENDS

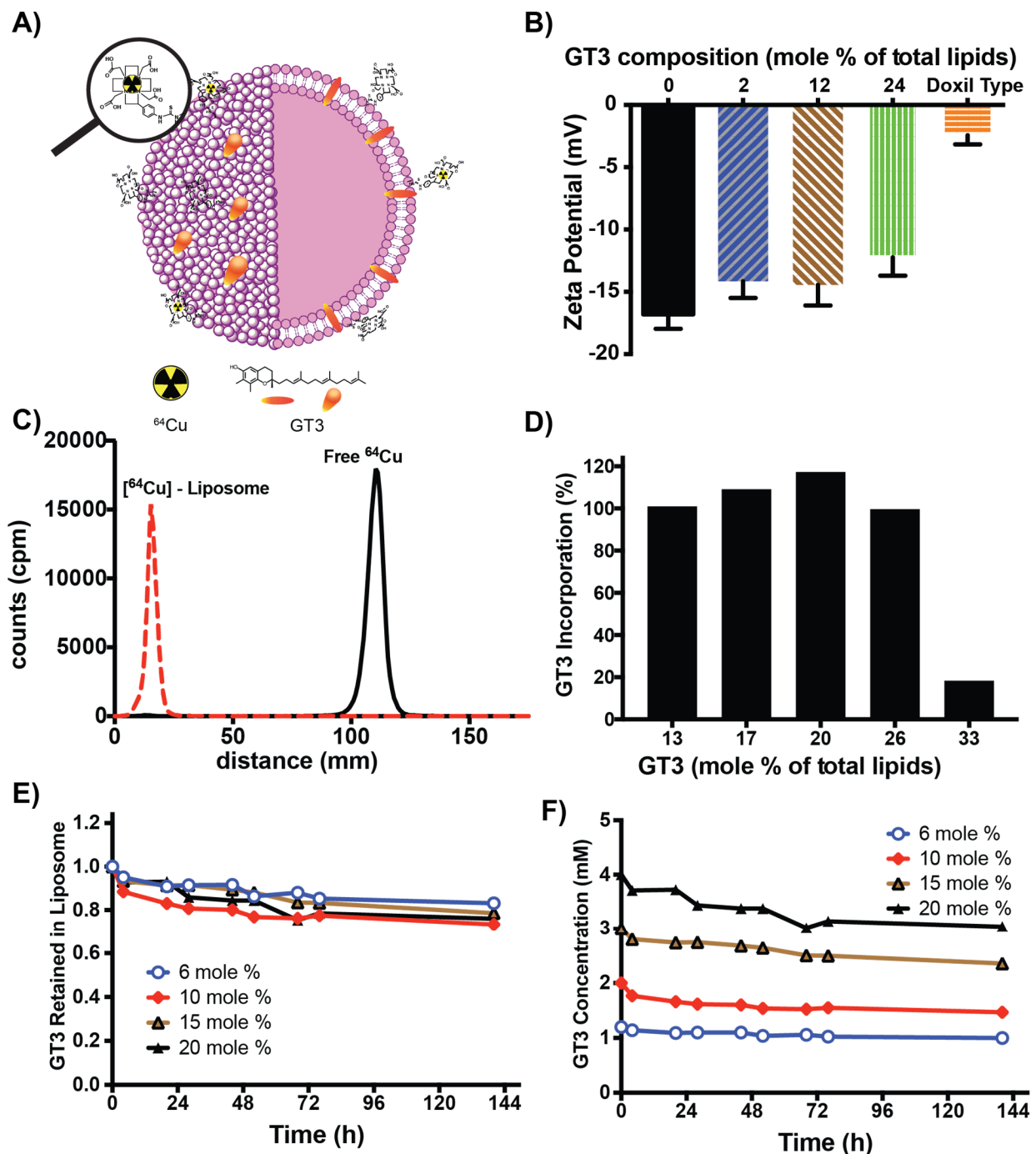


Fig. 1. Schematic and characterization of GT3-incorporated bone marrow targeting liposome. A) Structure of PET-labeled GT3-Nano. B) Zeta potentials of SBMT-LIPO. C) ^{64}Cu -GT3-NANO shows 100% labeling of ^{64}Cu on iTLC. D) GT3 incorporation into liposome. E, F) *In vitro* GT3 release kinetics

of GT3-Nano shows at 6, 10, 15, and 20 mole% GT3 contents in the liposome as relatively retained (E) and moles retained (F).

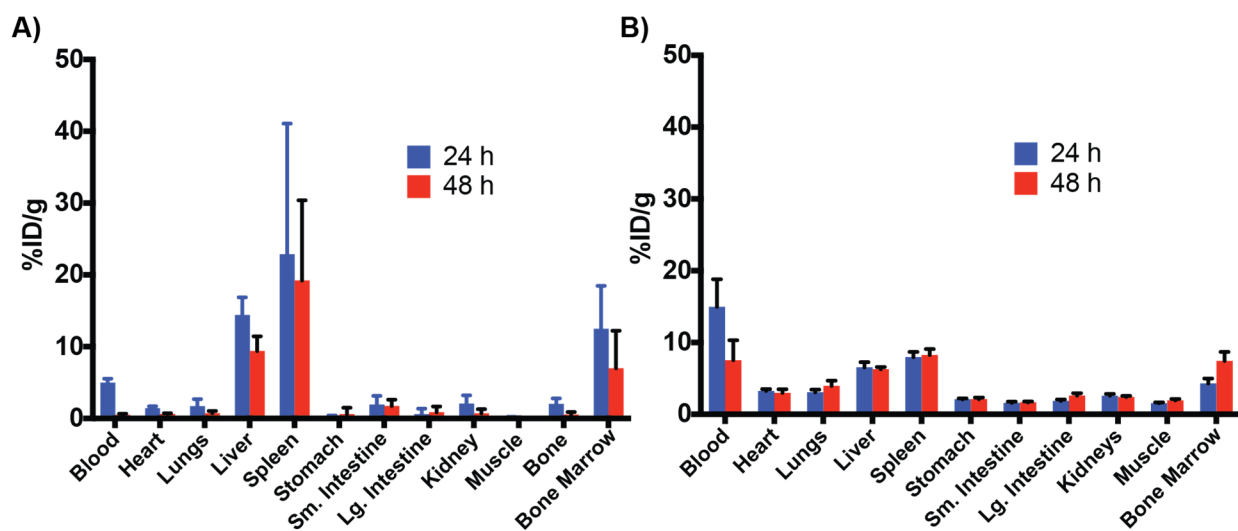


Fig. 2. Ex vivo biodistribution data. A) ^{64}Cu -labeled GT3-Nano and B) ^3H -GT3-Nano. The *ex vivo* biodistribution data of ^{64}Cu -labeled GT3-Nano and ^3H -GT3-Nano at 24 h and 48 h, respectively, is presented.

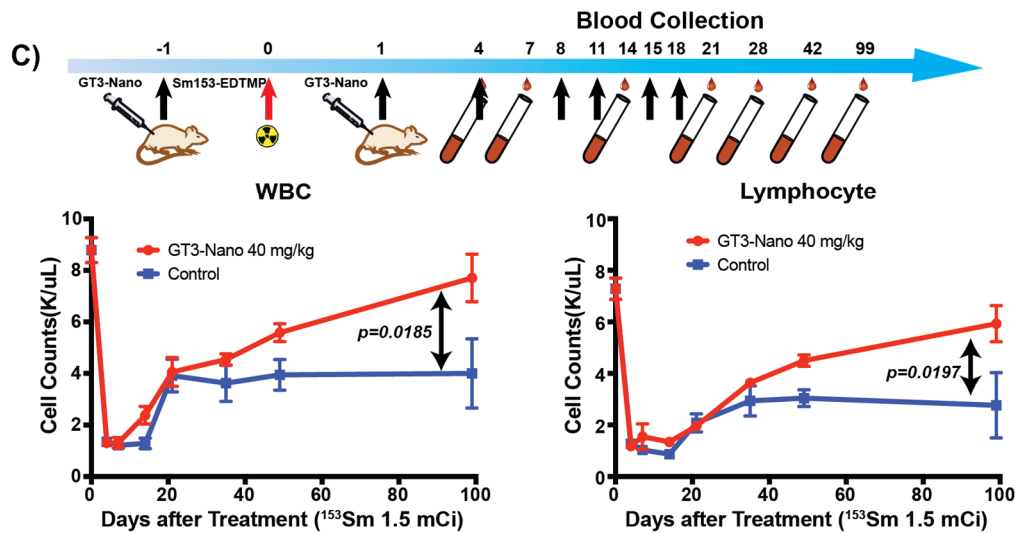
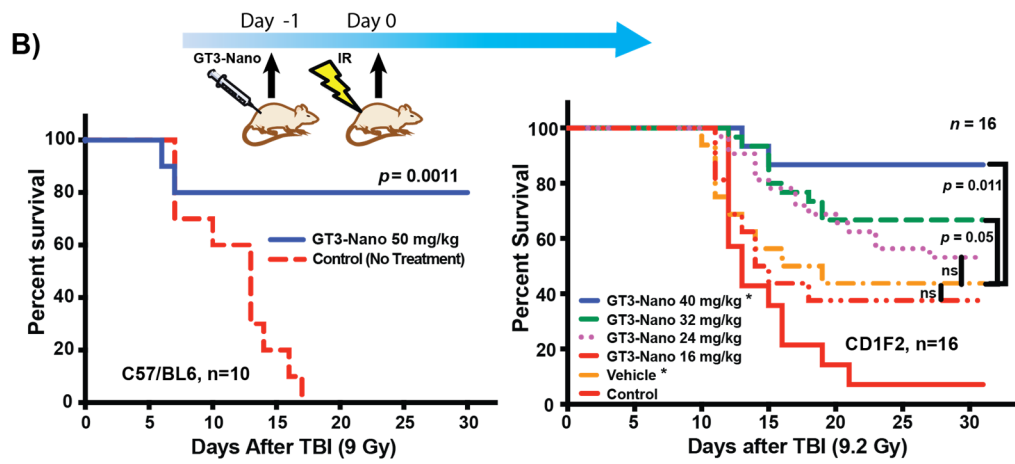
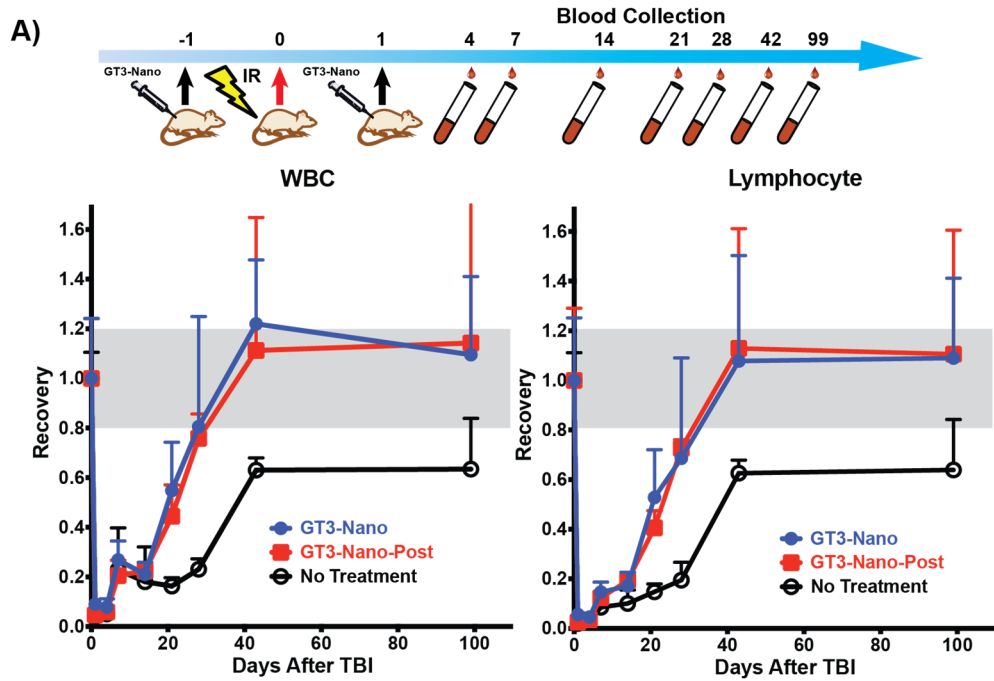


Fig. 3. Efficacy of GT3-Nano. A) WBC recovery after TBI (4 Gy) in 10 mg/kg/mice. B) Dose-dependent survival improvement of mice at lethal radiation doses. Left: C57/BL6 mice were administered GT3-Nano. Right: CD2F1 mice were administered GT3-Nano at various GT3 dosages and BMT-LIPO was given an equivalent amount of lipids to 40 mg/kg GT3-Nano. Data for control group (no treatment) was obtained from reference (12). C) WBC recovery of [¹⁵³Sm]-EDTMP treatment with GT3-Nano.

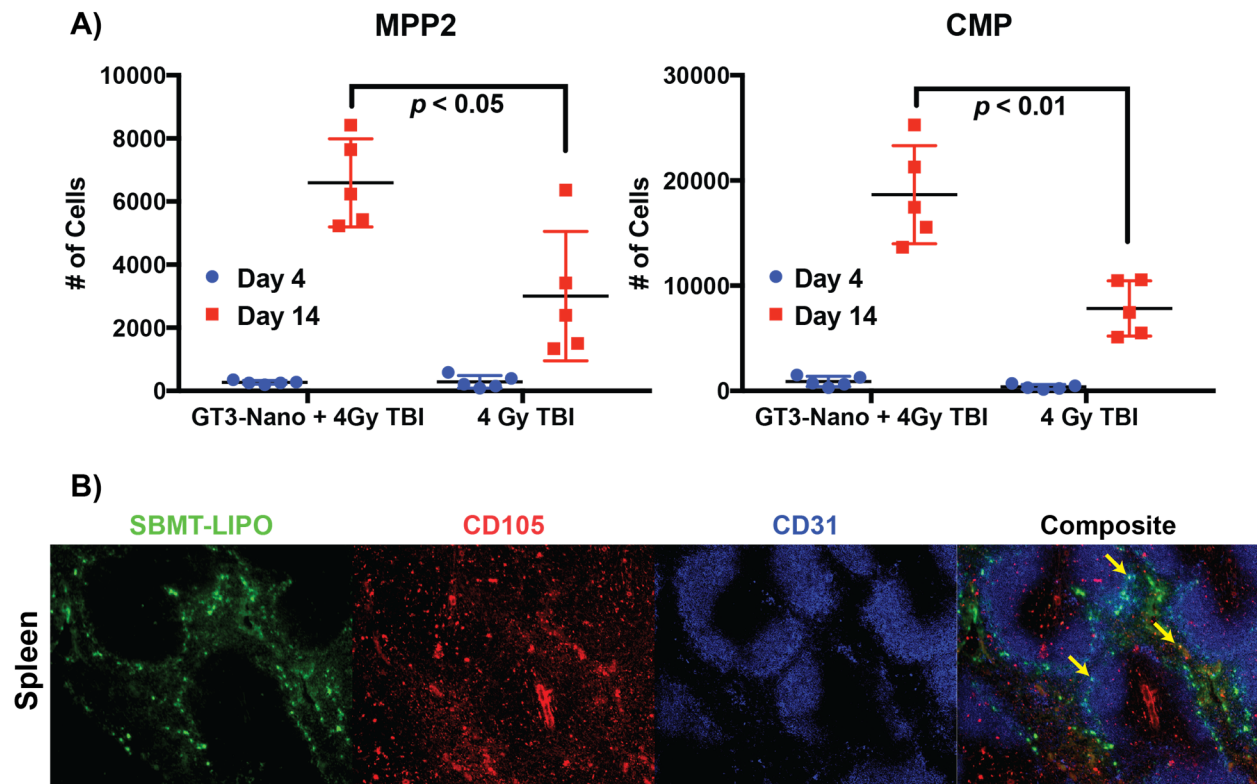


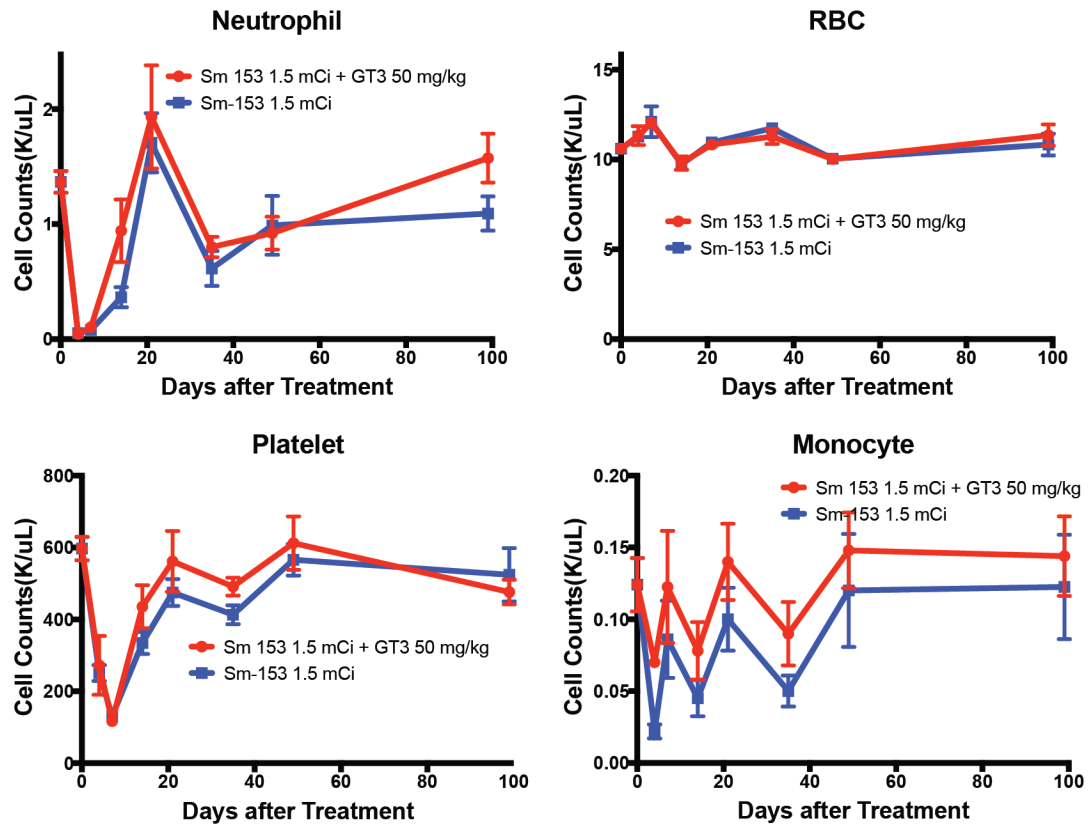
Fig. 4. A) GT3-Nano treated mice demonstrate improved recovery of HSC cell subpopulation changes in bone marrow with statistically significant increase in MPP2 and CMP. B) Immunohistochemistry of C57BL/6 mouse frozen spleen section. Composite imaging shows that SBMT-LIPO is co-localized mostly with CD105. There are a few regions (arrows) where SBMT-LIPO, CD105, and CD31 are co-localized.

REFERENCES

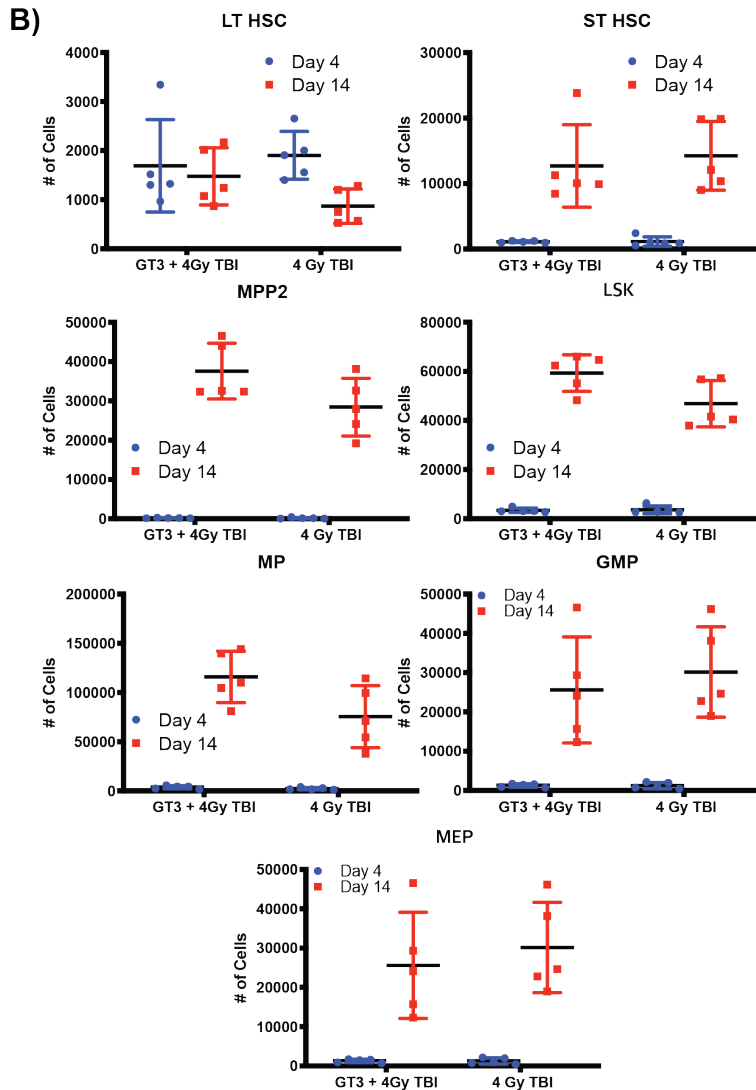
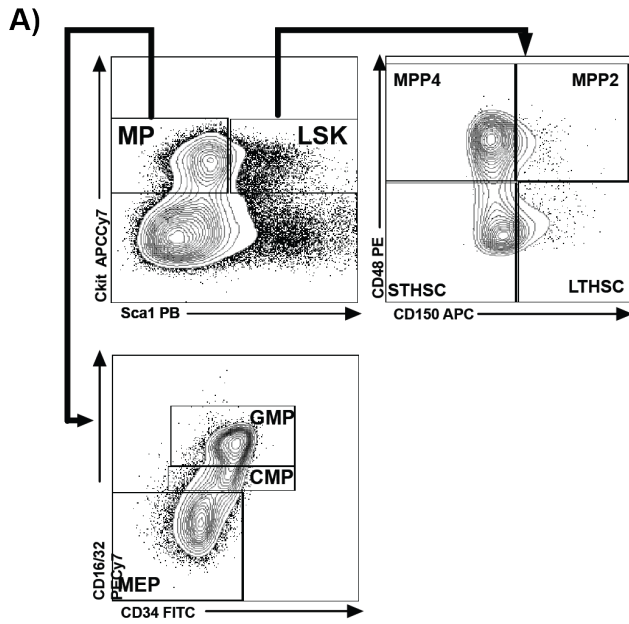
1. Moding EJ, Kastan MB, Kirsch DG. Strategies for optimizing the response of cancer and normal tissues to radiation. *Nat Rev Drug Discov.* 2013;12:526-542.
2. Worden F. Treatment strategies for radioactive iodine-refractory differentiated thyroid cancer. *Ther Adv Med Oncol.* 2014;6:267-279.
3. Pandit-Taskar N, Zanzonico PB, Kramer K, et al. Biodistribution and Dosimetry of Intraventricularly Administered (124)I-Omburtamab in Patients with Metastatic Leptomeningeal Tumors. *J Nucl Med.* 2019;60:1794-1801.
4. Bergsma H, Konijnenberg MW, Kam BL, et al. Subacute haematotoxicity after PRRT with (177)Lu-DOTA-octreotate: prognostic factors, incidence and course. *Eur J Nucl Med Mol Imaging.* 2016;43:453-463.
5. Bodei L, Modlin IM, Luster M, et al. Myeloid neoplasms after chemotherapy and PRRT: myth and reality. *Endocr Relat Cancer.* 2016;23:C1-7.
6. Nelp WB, Gohil MN, Larson SM, Bower RE. Long-term effects of local irradiation of the marrow on erythron and red cell function. *Blood.* 1970;36:617-622.
7. Strosberg J, El-Haddad G, Wolin E, et al. Phase 3 Trial of (177)Lu-Dotatate for Midgut Neuroendocrine Tumors. *N Engl J Med.* 2017;376:125-135.
8. Singh VK, Beattie LA, Seed TM. Vitamin E: tocopherols and tocotrienols as potential radiation countermeasures. *J Radiat Res.* 2013;54:973-988.
9. Nukala U, Thakkar S, Krager KJ, Breen PJ, Compadre CM, Aykin-Burns N. Antioxidant Tocols as Radiation Countermeasures (Challenges to be Addressed to Use Tocols as Radiation Countermeasures in Humans). *Antioxidants (Basel).* 2018;7.
10. Lee SG, Gangangari K, Kalidindi TM, Punzalan B, Larson SM, Pillarsetty NV. Copper-64 labeled liposomes for imaging bone marrow. *Nucl Med Biol.* 2016;43:781-787.
11. Ghosh SP, Kulkarni S, Hieber K, et al. Gamma-tocotrienol, a tocol antioxidant as a potent radioprotector. *Int J Radiat Biol.* 2009;85:598-606.
12. Singh VK, Wise SY, Fatanmi OO, et al. Progenitors mobilized by gamma-tocotrienol as an effective radiation countermeasure. *PLoS One.* 2014;9:e114078.

13. Tesio M, Tang Y, Mudder K, et al. Hematopoietic stem cell quiescence and function are controlled by the CYLD-TRAF2-p38MAPK pathway. *J Exp Med*. 2015;212:525-538.
14. Kenswil KJG, Jaramillo AC, Ping Z, et al. Characterization of Endothelial Cells Associated with Hematopoietic Niche Formation in Humans Identifies IL-33 As an Anabolic Factor. *Cell Rep*. 2018;22:666-678.
15. Liu D, Hu Q, Song YK. Liposome clearance from blood: different animal species have different mechanisms. *Biochim Biophys Acta*. 1995;1240:277-284.
16. Morrison SJ, Scadden DT. The bone marrow niche for haematopoietic stem cells. *Nature*. 2014;505:327-334.
17. Chen S, Epureanu B. Regular biennial cycles in epidemics caused by parametric resonance. *J Theor Biol*. 2017;415:137-144.
18. Nelp WB, Bower RE. The quantitative distribution of the erythron and the RE cell in the bone marrow organ of man. *Blood*. 1969;34:276-282.
19. Hooper AT, Butler JM, Nolan DJ, et al. Engraftment and reconstitution of hematopoiesis is dependent on VEGFR2-mediated regeneration of sinusoidal endothelial cells. *Cell Stem Cell*. 2009;4:263-274.
20. Azzam EI, Jay-Gerin JP, Pain D. Ionizing radiation-induced metabolic oxidative stress and prolonged cell injury. *Cancer Lett*. 2012;327:48-60.

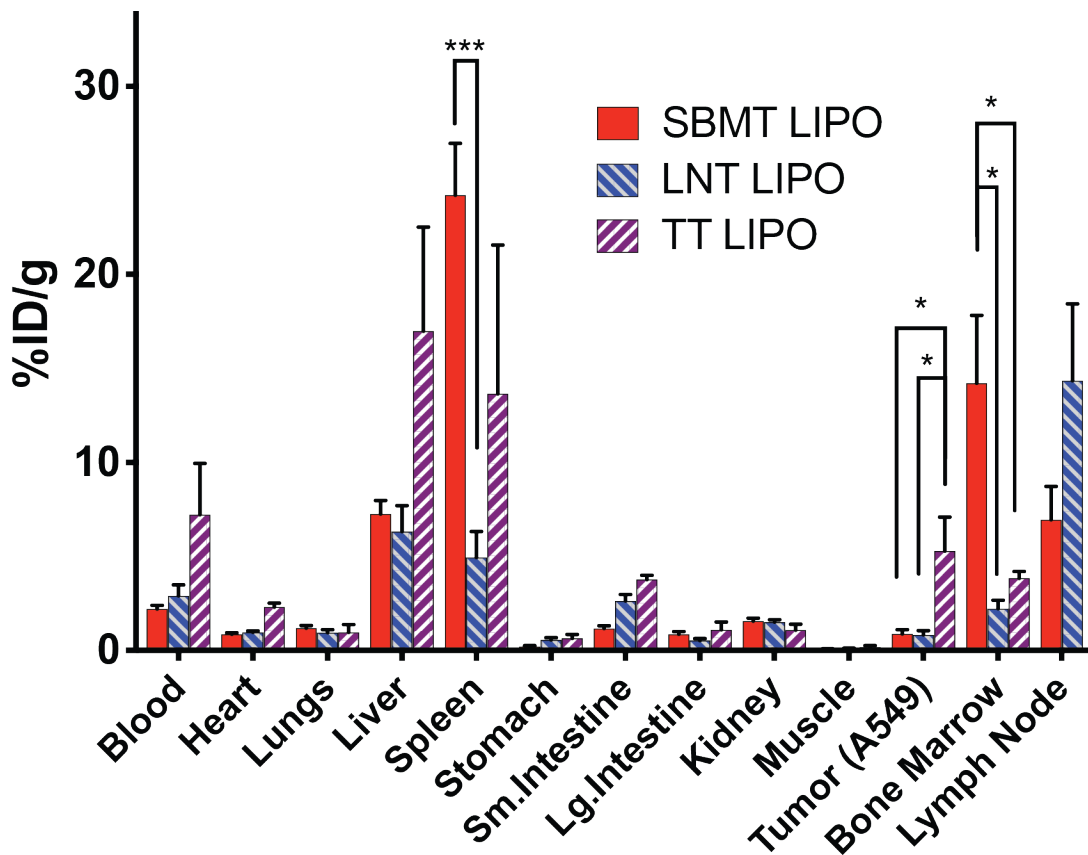
Supplementary Data



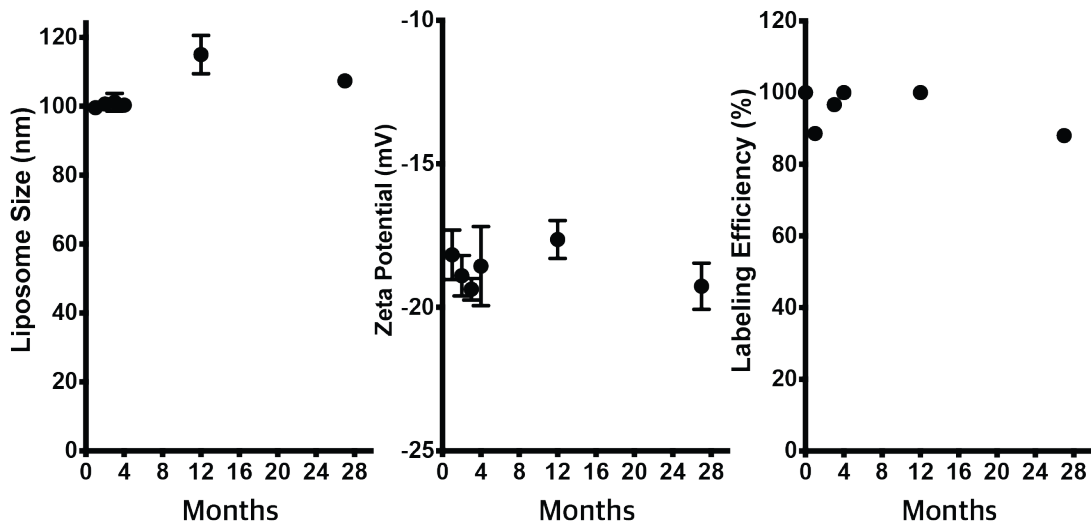
Supplemental Figure 1. Blood cell recovery of ^{153}Sm -EDTMP treatment with GT3-Nano. ^{153}Sm -EDTMP and GT3-Nano injection schedule and blood collection scheme: 1.5 mCi of Sm-153 was administered intravenously to two groups (5 mice per group) of mice. 40 mg/kg GT3-Nano was administered 24 h prior to ^{153}Sm -EDTMP injection and an additional 40 mg/kg GT3-Nano was administered on days 1, 4, 8, 11, 15, and 18. Blood was collected on days 4, 7, 14, 21, 28, 42, and 99. The data is presented as mean \pm SEM.



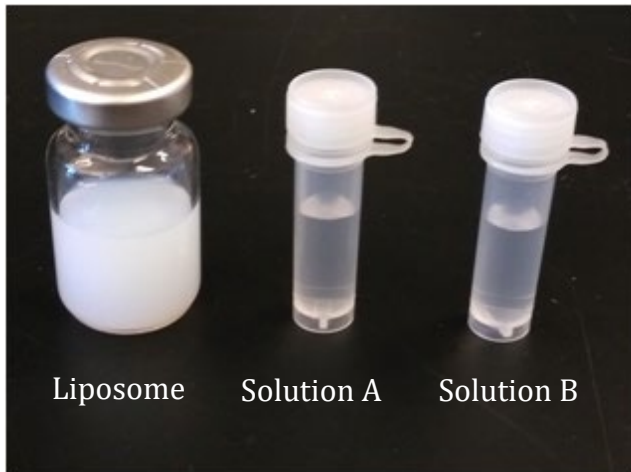
Supplemental Figure 2. HSC and HSPC cell population changes in bone marrow. A) gating strategy for HSPC (hematopoietic stem and progenitor cell) populations. B) After C57BL/6 mice were irradiated at 4 Gy with or without GT3-Nano, bone marrow was collected and analyzed by FACS. Myeloid-biased MPP subsets 2 (MPP2) and common myeloid progenitors (CMP) showed statistically significant recovery as compared to other HSPC and progenitor populations.



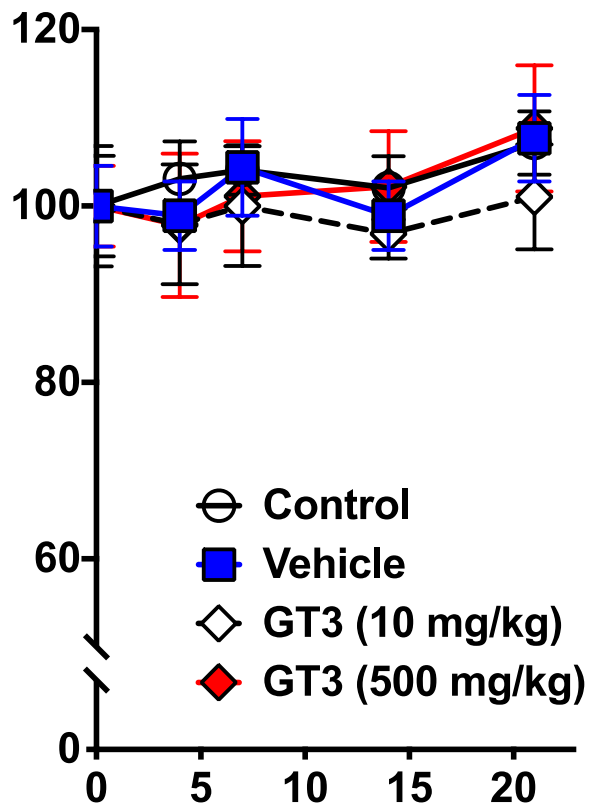
Supplemental Figure 3. Biodistribution of [⁶⁴Cu]-labeled selective targeting liposomes at 24 h post-injection. Athymic nude mice bearing A549 tumor were injected with ~140 μ Ci (5.18 MBq) of ⁶⁴Cu-labeled liposomes. 100 mg (2 μ moles) of lipid was injected into each mouse through *i.v.*, corresponding to approximately 6×10^{12} liposome particles per mouse. Mice were euthanized at 24 h post-injection and organs were harvested in pre-weighed tubes to measure organ weight and γ -counting. N=5 per group. Data was presented as mean and SEM. * $p < 0.05$, *** $p < 0.001$ SBMT: spleen and bone marrow-targeting liposomes; LNT: lymph node-targeting liposome; TT: tumor-targeting liposomes.



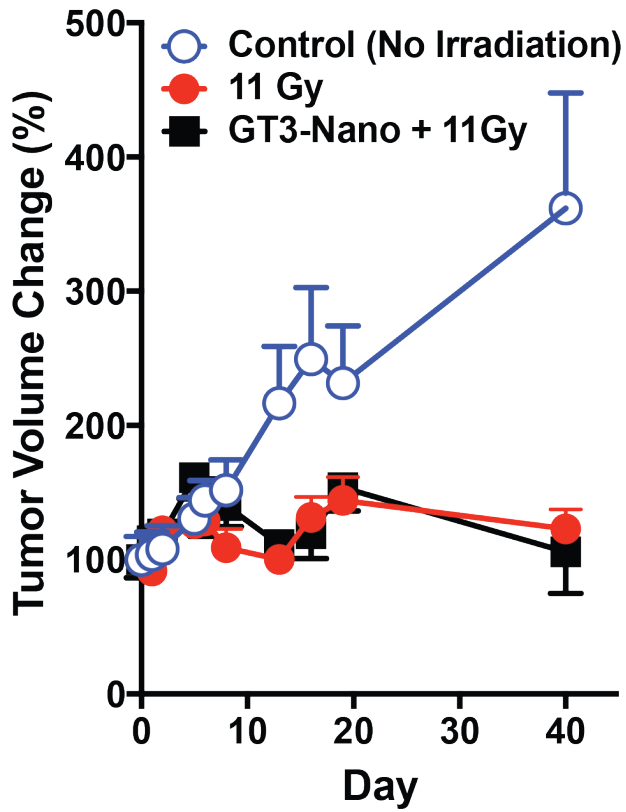
Supplemental Figure 4. SBMT-LIPO stability. SBMT-LIPO (20 mM total lipids) was stored at 4 °C and the size, zeta potential, and ^{64}Cu labeling efficiency was measured at 1, 2, 4, 6, 12, and 28 months. As seen above, SBMT-LIPO size, zeta potential, and labeling efficiency remain similar for 28 months.



Supplemental Figure 5. SBMT-LIPO as a “kit” formulation has been developed to label ^{64}Cu if needed. Solution A is 200 mM sodium acetate buffer (pH 5.0) and Solution B is 1 M NaOH. [^{64}Cu]-BMT-LIPO injection is prepared using the following aseptic procedure: Aseptically transfer 125 μL of solution A to 5 mL SBMT-LIPO vial at 50 $^{\circ}\text{C}$ and mix the solution by gentle swirling. Add aseptically desired activity of [^{64}Cu]- CuCl_2 into SBMT-LIPO vial and mix the solutions by gentle swirling. Place SBMT-LIPO vial in 50 $^{\circ}\text{C}$ heating block or heating bath for 30 minutes. Aseptically add 32 μL of neutralizing solution to BMT-LIPO vial. Labeling efficiency will be tested using iTLC with 5 mM DTPA.



Supplemental Figure 6. Body weight change with SBMT-LIPO and GT3-Nano. C57/BL6 mice were administered SBMT-LIPO (2.5 g/kg of total lipid) and GT3-Nano (10 mg/kg GT3 + 50 mg/kg total lipid or 500 mg/kg GT3 + 2.5 g/kg total lipid). Body weights of mice were monitored for 21 days. N=4 per group. Data is presented as mean \pm SD.



Supplemental Figure 7. GT3 Effect on Tumor with focal irradiation. 5×10^6 MDA-MB-468-LUC cells in 100 μ L Matrigel/PBS were injected s.c. to right flank of athymic nude mice. 5 mice per group. Tumor size became 50-100 mm^3 in two weeks and 10 mg/kg GT3 loaded liposomes were injected via i.v. 11 Gy was given to tumors using X-ray irradiator and tumor sizes were measured using caliper.

Supplemental Table 1. Biodistribution of GT3-loaded bone marrow-targeting liposomes labeled with [^3H]-GT3 and [^{64}Cu]-DOTA-Bn-DSPE. 5.5 MBq of ^{64}Cu -labeled GT3-Nano and 370 kBq of ^3H -labeled GT3-Nano were injected to mice *via* tail vein (n = 5 per group). Mice were sacrificed at the indicated time and major organs were collected and weighed. ^{64}Cu counting was done as soon as the organs were collected and ^3H counting was measured 5 days after the mice were sacrificed. The %ID/g was calculated by measuring weight and time-corrected measurement of radioactivity (n = 5 per group).

| | ^3H | | ^{64}Cu | |
|---------------|--------------|-------------|------------------|--------------|
| | 24 h | 48 h | 24 h | 48 h |
| Blood | 14.97 (8.85) | 7.54 (4.81) | 4.98 (0.25) | 0.50 (0.07) |
| Tumor (PC9) | N/A | N/A | 2.70 (0.36) | 0.74 (0.28) |
| Heart | 3.27 (0.47) | 2.98 (1.02) | 1.42 (0.12) | 0.62 (0.04) |
| Lungs | 3.07 (1.48) | 3.97 (1.45) | 1.72 (0.43) | 0.74 (0.13) |
| Liver | 6.53 (1.35) | 6.28 (0.63) | 14.40 (1.10) | 9.38 (0.92) |
| Spleen | 7.95 (1.61) | 8.26 (1.66) | 22.86 (8.14) | 19.20 (5.00) |
| Stomach | 2.09 (0.2) | 2.11 (0.45) | 0.20 (0.10) | 0.58 (0.41) |
| Sm. Intestine | 1.6 (0.3) | 1.66 (0.28) | 1.94 (0.54) | 1.74 (0.39) |
| Lg. Intestine | 1.87 (0.35) | 2.61 (0.66) | 0.60 (0.35) | 0.85 (0.41) |
| Kidney | 2.59 (0.46) | 2.41 (0.33) | 2.06 (0.51) | 0.72 (0.25) |
| Muscle | 1.53 (0.46) | 1.93 (0.39) | 0.14 (0.04) | 0.00 (0.00) |
| Marrow | 4.29 (3.22) | 7.44 (2.52) | 12.48 (2.68) | 6.98 (2.34) |

Supplemental Table 2. List of antibodies used for immunohistochemistry and flow cytometry.

| Antibody | Alternative names | Clone | Species | Company | Catalog Number |
|----------|-------------------|-------|---------|---------------|----------------|
| CD105 | Endoglin | poly | Rabbit | Abcam | ab107595 |
| CD31 | PECAM-1 | mono | Mouse | Abcam | ab24590 |
| Rb IgG | | poly | Goat | Abcam | ab150080 |
| Ms IgG | | poly | Goat | Abcam | ab150115 |
| CD3 | | mono | Hamster | eBioscience | 15-0031-83 |
| CD4 | | mono | Rat | eBioscience | 15-0041-83 |
| CD8 | | mono | Rat | eBioscience | 15-0081-83 |
| Gr1 | Ly6G/Ly6C | mono | Rat | eBioscience | 15-5931-82 |
| CD45R | B220 | mono | Rat | eBioscience | 15-0452-83 |
| CD19 | | mono | Rat | eBioscience | 15-0193-83 |
| Ter119 | CD253a | mono | Rabbit | eBioscience | 15-5921-82 |
| CD117 | c-Kit | mono | Rat | BioLegend | 105826 |
| Sca-1 | Ly6A/E | mono | Rat | BioLegend | 122520 |
| CD150 | SLAM | mono | Rat | BioLegend | 115910 |
| CD48 | BLAST-1 | mono | Hamster | BD Bioscience | 557485 |
| CD34 | RAM 34 | mono | Rat | eBioscience | 11-0341-85 |
| CD16/32 | Fcgr3/Fcgr2 | mono | Rat | BD Bioscience | 560829 |